



An automatic electronic instrument for accurate measurements of food volume and density

Ding Yuan¹, Xiaohui Hu¹, Hong Zhang¹, Wenyan Jia², Zhi-Hong Mao^{2,3} and Mingui Sun^{2,3,4,*}

¹School of Astronautics, Beihang University, Beijing, China: ²Department of Electrical & Computer Engineering, University of Pittsburgh, Pittsburgh, PA 15213, USA: ³Department of Bioengineering, University of Pittsburgh, Pittsburgh, PA 15213, USA: ⁴Department of Neurosurgery, University of Pittsburgh, Pittsburgh, PA 15213, USA

Submitted 30 October 2019: Final revision received 28 June 2020: Accepted 8 July 2020: First published online 28 August 2020

Abstract

Objective: Accurate measurements of food volume and density are often required as ‘gold standards’ for calibration of image-based dietary assessment and food database development. Currently, there is no specialised laboratory instrument for these measurements. We present the design of a new volume of density (VD) meter to bridge this technological gap.

Design: Our design consists of a turntable, a load sensor, a set of cameras and lights installed on an arc-shaped stationary support, and a microcomputer. It acquires an array of food images, reconstructs a 3D volumetric model, weighs the food and calculates both food volume and density, all in an automatic process controlled by the microcomputer. To adapt to the complex shapes of foods, a new food surface model, derived from the electric field of charged particles, is developed for 3D point cloud reconstruction of either convex or concave food surfaces.

Results: We conducted two experiments to evaluate the VD meter. The first experiment utilised computer-synthesised 3D objects with prescribed convex and concave surfaces of known volumes to investigate different food surface types. The second experiment was based on actual foods with different shapes, colours and textures. Our results indicated that, for synthesised objects, the measurement error of the electric field-based method was <1 %, significantly lower compared with traditional methods. For real-world foods, the measurement error depended on the types of food volumes (detailed discussion included). The largest error was approximately 5 %.

Conclusion: The VD meter provides a new electronic instrument to support advanced research in nutrition science.

Keywords
Food
Dietary assessment
Volume
Image
3D image reconstruction

With the high prevalence of obesity, diabetes and other chronic diseases, the study of caloric and nutritional intake becomes increasingly important^(1,2). Besides proper food choice, the control of portion size is the most deterministic factor in controlling intake. Traditionally, food portion size is measured in terms of either weight or volume. Although the weight measurement can be conducted precisely using a weighing scale, it is inconvenient because the weighing scale must be placed at, or carried to, the eating site. Volumetric portion size measurement, on the other hand, is traditionally conducted by self-estimation with reference to a common object (e.g. a cup, a spoon or a fist). In some cases, a set of descriptive terms is used (e.g. small, medium or large) instead of a quantitative volumetric value.

Although these intuitive approaches are easy to learn for people to self-monitor their intake, they are clearly very subjective and inaccurate. In addition, numerous studies have shown that people tend to underreport their intake^(3,4).

Recently, advances in microelectronics and mobile technology have led to an imaging approach to portion size measurement. A food image acquired by a cell phone or a wearable device can be used to quantitatively measure food volume based on a mathematical transformation of coordinates, expressed in matrices, between the image pixels and real-world coordinates^(5,6). Several computational methods have been developed^(7,8), including those based on wireframe shape models⁽⁹⁾, structured lights⁽¹⁰⁾ and

*Corresponding author: Email drsun@pitt.edu

© The Author(s), 2020. Published by Cambridge University Press on behalf of The Nutrition Society

depth maps^(11,12). Although this advanced imaging approach holds promise for objective portion size quantification, its accuracy is currently much lower than that of the weight-based approach. As a result, it is often required to assess volumetric accuracy before a large-scale dietary study is conducted. Unfortunately, one cannot assess this accuracy easily because the true volume of food that serves as the 'gold standard' is difficult to obtain. Traditionally, the water displacement method is often used to measure the true volume. However, foods that are destructible in water cannot be measured unless they are properly sealed. Frequently, the sealing process alters the volume if the food is compressible. Although water in this method can be replaced by certain plant seeds (e.g. rapeseeds or millets), sealing is still required for foods containing liquid, and the degree of seed compression, which is influenced by a variety of physical factors⁽¹³⁾, introduces a new source of error. Several advanced methods have been reported using a CT/MRI scan⁽¹⁴⁾ and a gas comparison pycnometer⁽¹⁵⁾. However, these methods are expensive, and they do not measure the same kind of volume as pictured in a photograph that shows only the surface of food, not its interior. Currently, the lack of accurate food volume measurement is a significant stumbling block in image-based dietary assessment.

Technological advances in dietetics and nutrition science face another significant challenge in updating the existing food databases. A food database for dietary assessment outputs values of calories and nutrients based on inputs of food names and portion sizes. Many currently used large databases were established over decades. Some food entries do not provide volumetric measures⁽⁷⁾. Updating food databases is thus necessary to support the new imaging technology. Clearly, this conversion cannot be accomplished properly without an accurate means to determine the true volume of food.

In this work, we present an electronic instrument to measure both food volume and density (VD). We call it a VD meter. The VD meter is composed of four main modules: a mechanical module to support a turning table and a weighing sensor; a camera module for image acquisition by an array of cameras with illuminating lights; an electronic module for power supply and system control/coordination; and a data processing module for performing image calibration and 3D surface reconstruction.

The rest of the paper is organised as follows. The structural design of the VD meter will be described. The subsequent section highlights our algorithms for image calibration and reconstruction with an emphasis on a new mathematical model that mimics the physical properties of the electric field. We use this model to estimate food surface from a 3D point cloud, followed by estimating the volume and density. Our experiments and data analysis will be presented. After a discussion about several important constraints in food volume measurement, this paper will be concluded.

Structural and hardware design

A cross-sectional view (in the vertical direction) of the VD meter is illustrated in Fig. 1. The mechanical module contains a turntable rotating precisely at a constant speed of 0.625 rpm and driven by a step motor through a transmission system. A high-precision load sensor is installed under the turntable as the weighing sensor. The camera module of the VD meter contains an arc-shaped stationary support that is installed with a set of high-quality cameras (Type MER-132-30GM; Daheng Group, Inc.) with a resolution of 1292×964 pixels, frame rate 30 frames per second and pixel size of $3.75 \times 3.75 \mu\text{m}$. In our experiment, we used three cameras (installed on the arc support and marked with green borders), and the imaging rate was sixty-four images per turntable rotation. The cameras are properly angled towards the turntable. The support arc is also installed with a set of white LED aiming at the turntable. Each LED is located at the middle of the neighbouring cameras. The electronic module within the VD meter provides power to other units, interfaces data (for cameras, weighing sensor and exterior computer) and coordinates functions among other system components. Additionally, a data processing module, which is a set of software, is loaded in both the microcomputer within the VD meter and a desktop computer connected to the VD meter. The assembled system is shown in Fig. 2a.

During measurement, food, with or without a plate, is placed on top of the turntable. The control unit has an option to tare the plate weight automatically to obtain the net weight of the food. As the turntable rotates for an entire cycle (360°), the set of cameras synchronously takes images at multiple positions, forming an imaging surface shaped like a mesh dome food cover (Fig. 2b). Precisely, sixty-four images were taken for each camera, and a total of $64 \times 3 = 192$ images were obtained by the three cameras of the VD meter for each food measurement. Since the rotation speed of the turntable and the locations/orientations of the cameras are known, all picture-taking points (small red cameras in Fig. 2b) on the 'mesh dome' are known and distributed regularly on the dome, minimising the likelihood

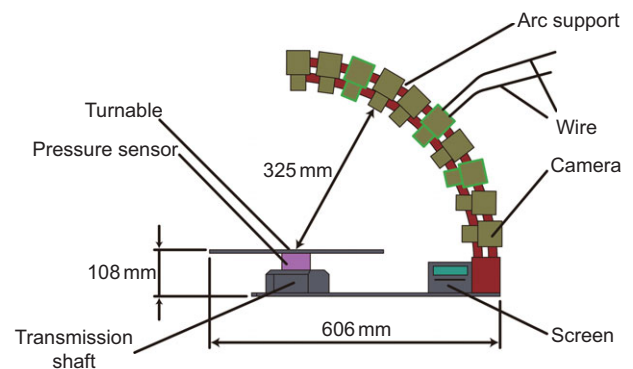


Fig. 1 (colour online) Food image acquisition platform

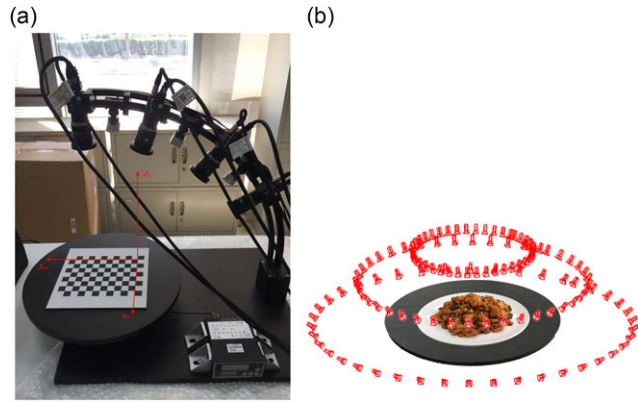


Fig. 2 (colour online) (a) A VD meter assembly with the world coordinate system indicated (in red colour); (b) imaging surface and equivalent image-taking points (small red cameras)

of occlusion. With shadowless illumination provided by white LED, the VD meter provides an imaging platform for high-accuracy food image reconstruction. Here we note that the size of the food measurable by the VD meter is limited by the turntable size and the space within the imaging area. However, we intentionally designed them to be sufficiently large (Fig. 2a) for common foods.

System calibration and volume estimation based on 3D point cloud

System calibration

In order to establish correspondences between image pixels and real-world coordinates, the imaging system within the VD meter must be calibrated. This calibration is required only once if the system is not re-adjusted or repositioned. The calibration is performed using an algorithm (more information is provided in Supplementary material S1) with a sheet of checkerboard placed on the turntable, as shown in Fig. 2.

Point cloud construction from multi-view images

The purpose of this part of the algorithm is to compute a 3D cloud of food surface points based on 192 2D images in different views. While the details of the algorithm can be found in Supplementary material S2, here we highlight the key procedures utilised. First, a set of common points (called feature points) observable from multiple neighbourhood images are selected automatically. Then, these feature points are one-to-one registered across as many images as possible. Next, the 3D relationships of these feature points are obtained and utilised to calculate a 3D cloud of points in the actual world coordinates (in a real-world unit, e.g. millimetre) as illustrated in Fig. 3. Finally, outlier points due to noise are identified and removed from the point cloud.

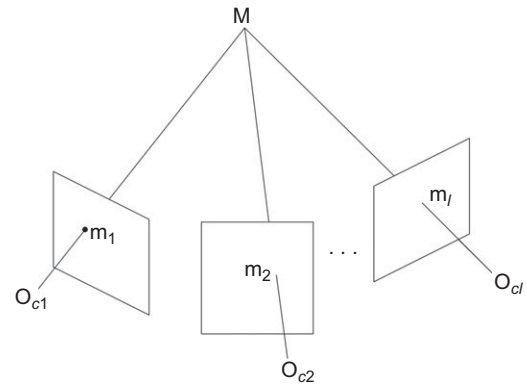


Fig. 3 Principle of 3D point reconstruction

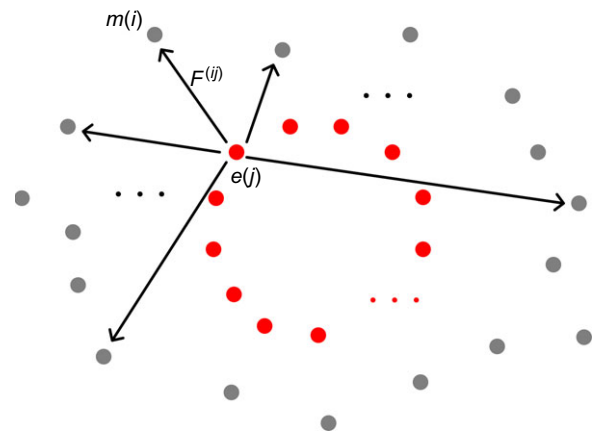


Fig. 4 (colour online) Model of the electric field-based method

Volume estimation from point cloud

The next major computational procedure is to estimate food volume from the point cloud. Traditionally, this estimation is performed using the convex hull method in which the surface is assumed to be locally convex^(16,17). However, it is problematic to estimate the food volume using this method because this special type of 3D objects often has concave local surfaces. When the convex hull method is applied to a concave surface, the estimated volume tends to be larger than the true volume. In order to solve this significant problem, we present two methods for food volume estimation: a simple sliced point cloud method and a robust estimation method using a new electric field-based physical model (Fig. 4). These methods are described in detail in Supplementary material S3.

Experiments

To evaluate the performance of the VD meter, we conducted two experimental studies of both computer-synthesised 3D objects and real food samples. Since the food density is equal to mass divided by volume, and the mass measurement is at least two orders of magnitude

more accurate (when a high-quality digital load sensor is used) than the volumetric measurement, the error in mass measurement can be ignored. As a result, the accuracy of volumetric measurement is equivalent to the accuracy of density measurement. Therefore, we needed only to perform experiments for the volumetric case. We used computer synthesis in the first study because, in this case, the true volumes of 3D objects are precisely known, and this approach allows us to evaluate our algorithm performance for specific concave surfaces. In the second study, real-world food samples with a variety of shapes, colours and textures were utilised to evaluate the VD meter performance. In both studies, we compared volume estimation accuracies of different methods, including the convex hull method, the slice-based method and the electric field method. For the last method, we conducted an additional study by changing point cloud density and adding noise and outliers to evaluate the robustness of this method.

Experiments on synthetic object models

Two 3D volumetric models were synthesised computationally, as shown in Fig. 5. We applied the convex hull method, slice-based method and electric field method to each point cloud for volume estimation and compared their results against the ground truth volumes of synthesised models. We performed the slice-based method twice for

$N=10$ and $N=18$, where N represents the number of slices.

Table 1 compares the three methods quantitatively, where both $N=10$ and $N=18$ cases for the slice-based method are listed. It can be observed that the convex hull method tends to distort the regions where the object surface is locally concave. As a result, the estimated volumes are larger than the true volumes (comparing Figs. 5 and 6). In contrast, in our electric field-based method, the point cloud points were well fit by the free particles even in concave regions (Fig. 7).

Compared with the convex hull method, the accuracy of the electric field method is higher. In the slice-based method, estimation accuracy tends to increase as the number of slices increases. However, this method has a significant problem: it is difficult to determine N (number of slices) applicable to different point cloud models. For a specific food, N needs to be adjusted manually. Estimation accuracy tends to increase as the number of slices increases, but, if the number of slices is too large, the number of points in each slice reduces, which tends to affect estimation accuracy negatively.

For the best performing electric field method, we conducted additional experiments to evaluate its robustness by changing the density of the original point cloud. For each object model, we compared three point cloud densities, as shown in Table 2. It can be observed that

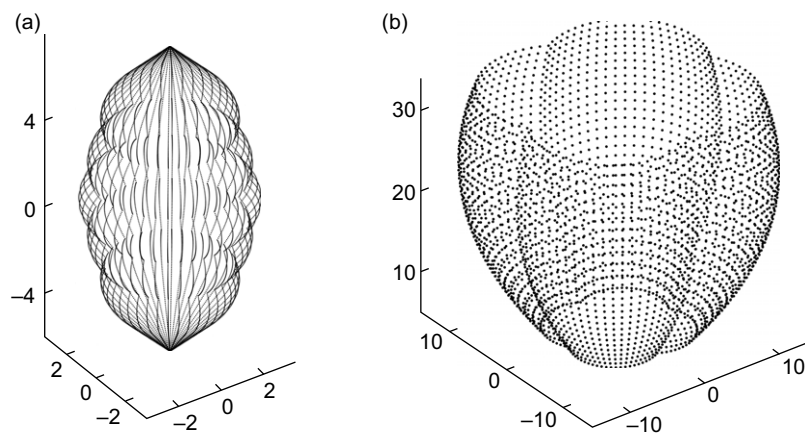


Fig. 5 Original point cloud of synthetic 3D object models: (a) model 1; (b) model 2

Table 1 Volume estimation results of synthesised object models

	Convex hull-based method	Slice-based method ($n=10$)	Slice-based method ($n=18$)	Electric field-based method
Model 1 (ground truth = 279.2 cm ³)				
Estimated volume (cm ³)	294.2	291.7	286.1	277.6
Error	5.4 %	4.5 %	2.5 %	0.6 %
Model 2 (ground truth = 1802.3 cm ³)				
Estimated volume (cm ³)	1839.4	1839.6	1836.7	1819.2
Error	2.1 %	2.1 %	1.9 %	0.9 %

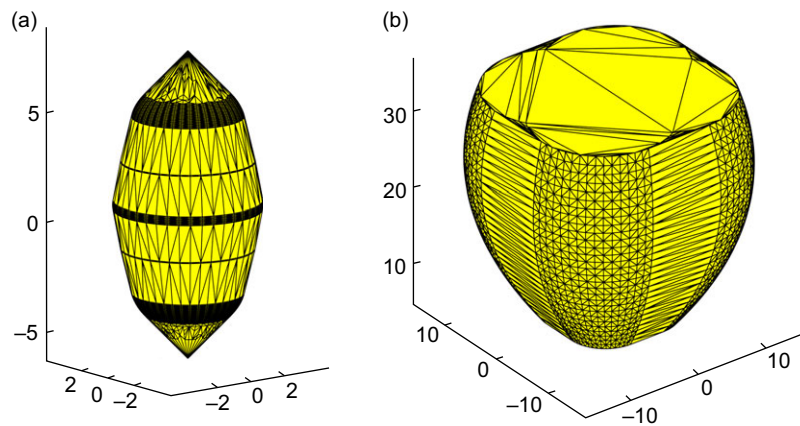


Fig. 6 (colour online) Estimation of the convex hull method for volumetric models in Fig. 5: (a) model 1; (b) model 2

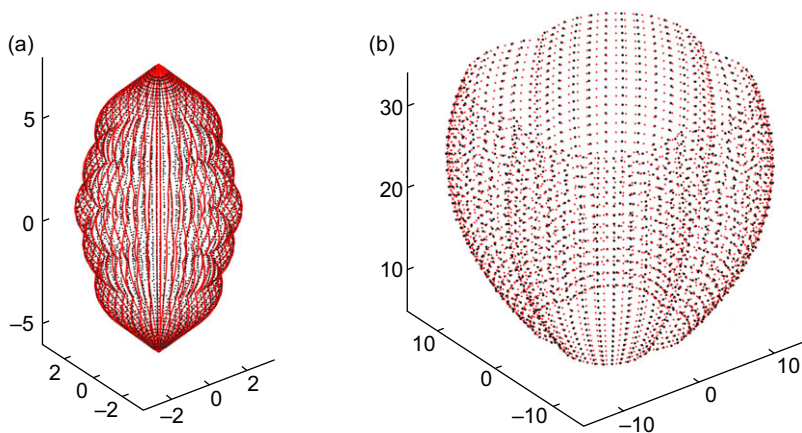


Fig. 7 (colour online) Estimation of the electric field method for volumetric models in Fig. 5: (a) model 1; (b) model 2

Table 2 Volume estimation results of the electric field method with different densities

	Model 1 (ground truth = 279.2 cm ³)			Model 2 (ground truth = 1802.3 cm ³)		
Number of points	5880	11 480	17 220	4304	6049	12 007
Ground truth (cm ³)	279.2	279.2	279.2	1802.3	1802.3	1802.3
Estimated volume	278.5	277.6	278.1	1819.2	1802.4	1797.9
Error	0.3 %	0.6 %	0.4 %	0.9 %	0.006 %	0.2 %

estimation accuracy remains <1 % regardless of the choices of number of points in the cloud. During 3D reconstruction, noisy outliers are present due to calibration error, matching error and other sources of errors. These outliers are often difficult to remove. In order to evaluate the electric field method with the presence of noise and outliers, we added white Gaussian noise (mean = 0, standard = 1) and outliers (randomly generated from a uniform distribution in the range of [0.05, 5]) separately to each point cloud and performed volume estimation. The results (Table 3) indicate that the electric field method maintained similar performances regardless of noise and outliers.

Experiments on real food samples

Six foods, purchased from cafeteria and food stores, were used to study the real-world performance of the VD meter. For each food, we used the VD meter and applied the electric field method to estimate the volume. For the same food, we also obtained its 3D point cloud using a laser scanner⁽¹⁸⁾, which is considered to be close to the ground truth of 3D shape of the food. The electric field method is also applied to the 3D point cloud from the laser scanner to estimate the volume, in order to check the accuracy of 3D point cloud from the VD meter. Furthermore, we also used the slice-based method, where both $N=20$ and $N=50$

Table 3 Volume estimation results of the electric field method with added noise and outliers to point clouds

	Original point cloud	Point cloud with random noise	Point cloud with outliers
Model 1 (ground truth = 279.2 cm ³)			
Estimated volume (cm ³)	277.5	296.0	283.0
Error	0.6 %	6.0 %	1.4 %
Model 2 (ground truth = 1802.3 cm ³)			
Estimated volume (cm ³)	1819.2	1817.6	1817.2
Error	0.9 %	0.8 %	0.8 %

were implemented. Finally, water displacement (manual measurement) was adopted as a base for comparison, as it is a very traditional and 3D-point-free method to obtain the food volume.

We first performed system calibration to establish correspondences between image pixels and real-world coordinates using a commercial, high-precision checkerboard. Then, 192 images (taken by three cameras) of foods in different views were produced by the VD meter. Next, feature points were detected using combined features of Harris⁽¹⁹⁾ and features from accelerated segment test (FAST)⁽²⁰⁾ and speeded-up robust features (SURF)⁽²¹⁾ as described in Supplementary material S2. The threshold value of T_{\min} was experimentally chosen to be 3. Then, the point cloud of each shape model was computed according to Eq. (7) in the Supplementary material. To remove noise and outliers, we filtered raw clouds using $K_p = 10$. After filtering, we applied the electric field method to reconstruct the surface for each food and estimating its volume.

In contrast to the VD meter, the number of points obtained by the laser scanner was very large (usually on the order of 10^5). As a result, estimating the volume directly using the raw point cloud data was time-consuming. Since the density of the point cloud has only limited effect on volume estimation accuracy, to accelerate computation, the original laser point cloud was down-sampled 80 % for volume estimation.

Table 4 lists the names of real foods (column 1), results based on water displacement method (column 2, which was used as the base for comparison), results of slice-based method with its corresponding errors (columns 3 and 4 for

$N = 20$ and columns 5 and 6 for $N = 50$), image-based electric field method with its corresponding errors (columns 7 and 8) and laser-based electric field method with its corresponding errors (columns 9 and 10) and cubic centimetre as the unit of estimation values. The number of 3D points in the real food study ranges from 7000 to 20 000.

Several important observations can be made from Table 4. First, our electric field-based method achieved better performance than the slice-based method. Although the best number of slices can be found for optimising volume estimation, the optimal number differed between foods. Second, the electric field method achieved satisfactory performance regardless of different food shapes both in image-based and laser-based point clouds.

Figure 8 shows food images tested (first row) and their experimental results using both image- (second row) and laser- (third row) based electric field methods. In the bottom two rows, red and green points represent, respectively, food point clouds (i.e. particles in the *PCP* set) and the final positions of free particles in the *NCP* set. It can be seen that the green points well represent the surfaces of red food point clouds.

All the experiments were performed using a computer equipped with Intel Core i7 3.5 GHz CPU and 16 GB RAM. The time required for each measurement depends on the complexity of food shapes and the number of points reconstructed to estimate the volume. In our analysis, the typical amount of time ranges from 3 to 5 min using MATLAB. We expect the duration to be shortened substantially using a different code, but with additional programming effort.

Table 4 Different methods of volume estimation of real foods

	Water displacement method (cm ³)	Slice-based method (n 20, cm ³)		Slice-based method (n 50, cm ³)		Image-based electric field method		Laser-based electric field method	
		Volume (cm ³)	Error	Volume (cm ³)	Error	Volume (cm ³)	Error	Volume (cm ³)	Error
Burger	540	352	34.8 %	396	26.7 %	530	1.85 %	558	3.33 %
Bread	488	396	18.9 %	416	14.8 %	477	2.25 %	473	3.07 %
Apple	242	198	18.2 %	213	12.0 %	244	0.83 %	221	8.70 %
Rice	180	157	12.8 %	171	5.0 %	178	1.11 %	186	3.33 %
Salad	185	159	14.1 %	167	10.0 %	179	3.24 %	191	3.24 %
Stir fry	153	140	8.5 %	158	3.3 %	145	5.23 %	159	3.92 %

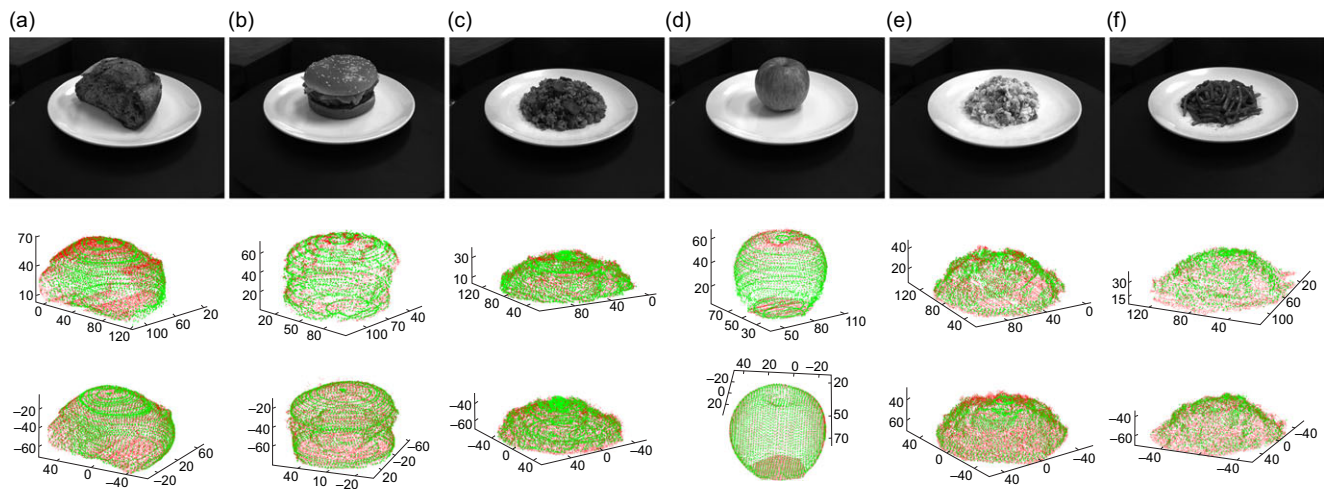


Fig. 8 (colour online) Point cloud fitting results of real foods. Top row is the set of original food images. Point clouds of the image-based electric field method and the laser-based electric field method are shown in the middle and bottom rows, respectively. Red points represent the food point cloud (points in the PCP set) acquired via the image or laser method, and green points represent the final positions of points in the NCP set: (a) bread, (b) burger, (c) rice, (d) apple, (e) salad, (f) dish

Discussion

Since the VD meter measures food volume and density, it is necessary to discuss the physical definitions of these quantities and several important challenges regarding their measurements. Unlike numerous incompressible objects in the physical world that have no ambiguity in their volumetric measures, foods do not have a unique definition for its volume. For example, the volume of an apple or a cup of coffee is well defined. However, the volume of a bowl of rice or a plate of salad is ambiguous because these compressible objects are porous with connected air spaces and, as a result, the boundary between food and air is uncertain. Strictly speaking, volumetric measurement of this type of food is not a deterministic quantity, but rather a probability distribution! In order to mitigate this fundamental problem, three kinds of food volumes (and densities) have been defined⁽²²⁾: bulk volume, apparent volume and net volume. Bulk volume is the volume defined by the container (e.g. a box of cereal); apparent volume is defined by a hypothetical enclosure covering the food; and net volume, which cannot be measured using a camera, is the volume of net matter excluding all spaces. Despite these three definitions, food volume is still an ambiguous quantity. A bowl of non-liquid food has both bulk and apparent volumes (e.g. the top and bottom parts of the food in a bowl fit the definitions of apparent and bulk volumes, respectively). A compressible food in a bowl or plate does not have the same volume precisely if measured twice. This phenomenon is due partially to the redistribution of food elements and the variation of ‘tightness’ of the hypothetical enclosure. Similarly, the concept of ‘spaces’ cannot be accurately defined in the net volume because new gaps between matters or particles always exist as we descend into a lower scale of observation. Therefore, we must accept the

ambiguity in food volume (density as well) and treat these quantities with a certain level of uncertainty (we emphasise, again, they are probability distributions). As a result, an overly high requirement for ‘accuracy’ in the volume of a compressible food is unnecessary and misleading. By the same token, volume and density measurements using the VD meter are ‘accurate’ only relevant to the average physical states of foods being served in the real world, including its usual amount of water content, temperature, surrounding pressure and commonly accepted containers. Moreover, the VD meter only measures the average density of the entire food, not its local density.

Conclusion

In this paper, we presented a new instrument, the VD meter, to measure both food volume and density. This instrument contains a number of hardware and software modules, including a turntable, a pressure sensor, an array of cameras, an array of illumination lights, an electronic circuitry for system control functions and a set of software performing computations. We also presented a new algorithm to estimate the 3D surface from a point cloud based on a physical model that governs the motions of charged particles in an electric field. This model produces a 3D surface of food which can have both convex and concave local regions. Our experiments using both synthesised and real foods indicate that the electric field method overperforms the reference methods for food volume estimation. The VD meter presented in this paper provides a new tool for both portion size estimation in dietary studies and the improvement of food databases.



Acknowledgements

Acknowledgements: The authors would like to acknowledge all the participants for their significant contributions to this research study, as well as Hao Ma for collecting experimental data. **Financial support:** This work was supported in part by the State's Key Project of Research and Development Plan in China (H. Z., D. Y., M. S., W. J., grant no. 2016YFE0108100), the National Institutes of Health grants (R01CA165255, R21CA172864 and R56DK113819) and the Bill & Melinda Gates Foundation (contract ID OPP1171395). **Conflicts of interest:** None. **Authorship:** D. Y., X. H. and H.Z. were responsible for camera calibration/image collection/analysis. D. Y., X. H., H.Z., W.Y. and M.S. contributed to the algorithm for data analysis. D. Y., X. H., H.Z., W.Y., Z.M. and M.S. contributed to final drafting and editing of the manuscript. **Ethics of human subject participation:** The experiment of this research measures volume and density of the food, It does not involve any human subjects.

Supplementary material

For supplementary material accompanying this article visit <https://doi.org/10.1017/S136898002000275X>

References

1. Bray GA & Popkin BM (1998) Dietary fat intake does affect obesity! *Am J Clin Nutr* **68**, 1157–1173.
2. Celis-Morales C, Lyall D, Gray S *et al.* (2017) Dietary fat and total energy intake modifies the association of genetic profile risk score on obesity: evidence from 48 170 UK Biobank participants. *Int J Obes* **41**, 1761–1768.
3. Gemming L, Jiang Y, Swinburn B *et al.* (2014) Under-reporting remains a key limitation of self-reported dietary intake: an analysis of the 2008/09 New Zealand adult nutrition survey. *Europ J Clin Nutr* **68**, 259–264.
4. Maurer J, Taren D, Teixeira P *et al.* (2006) The psychosocial and behavioral characteristics related to energy misreporting. *Nutr Rev* **64**, 53–66.
5. Zhang Z, Yang Y & Yue Y (2011) Food volume estimation from a single image using virtual reality technology. In Proceedings of the IEEE 37th Annual Northeast Bioengineering Conference (NEBEC), pp. 1–2.
6. Gao A, Lo FPW & Lo B (2018) Food volume estimation for quantifying dietary intake with a wearable camera. In Proceedings of the IEEE International Conference on Wearable and Implantable Body Sensor Networks (BSN), pp. 110–113.
7. Weiss R, Stumbo PJ & Divakaran A (2010) Automatic food documentation and volume computation using digital imaging and electronic transmission. *J Am Diet Assoc* **110**, 42–44.
8. Jia W, Li Y, Qu R *et al.* (2019) Automatic food detection in egocentric images using artificial intelligence technology. *Public Health Nutr* **22**, 1168–1179.
9. Jia W, Chen HC, Yue Y *et al.* (2014) Accuracy of food portion size estimation from digital pictures acquired by a chest-worn camera. *Public Health Nutr* **17**, 1671–1681.
10. Makhssous S, Mohammad HM, Schenk JM *et al.* (2019) A novel mobile structured light system in food 3D reconstruction and volume estimation. *Sensors* **19**, 564.
11. Fang S, Zhu F, Jiang C *et al.* (2016) A comparison of food portion size estimation using geometric models and depth images. In Proceedings of the IEEE International Conference on Image Processing, pp. 26–30.
12. Lo FP, Sun Y, Qiu J *et al.* (2018) Food volume estimation based on deep learning view synthesis from a single depth map. *Nutrients* **10**, 2005.
13. Lupu M, Canja CM & Padureanu V (2014) The analyses of the cereal grains mechanical properties. In Proceedings of the International Conference Research and Innovation in Engineering, pp. 280–283.
14. Kelkar S, Boushey CJ & Okos M (2015) A method to determine the density of foods using x-ray imaging. *J Food Eng* **159**, 36–41.
15. Sereno AM (2007) Determination of particle density and porosity in foods and porous materials with high moisture content. *Int J Food Prop* **10**, 455–469.
16. Preparata FP & Hong SJ (1977) Convex hulls of finite sets of points in two and three dimensions. *Commun ACM* **20**, 87–93.
17. Li Z, Wang K, Jia W *et al.* (2015) Multiview stereo and silhouette fusion via minimizing generalized reprojection error. *Image Vision Comput* **33**, 1–14.
18. Wang J, Zhang J & Xu Q (2014) Research on 3D laser scanning technology based on point cloud data acquisition. In Proceedings of the International Conference on Audio, Language and Image Processing (ICALIP), Shanghai, China, 7–9 July 2014, pp. 631–634. New York: Institute of Electrical and Electronics Engineers; available at <https://ieeexplore.ieee.org/document/7009871/> (accessed August 2020).
19. Harris C & Stephens M (1988) A combined corner and edge detector. In Proceedings of Alvey Vision Conference, Manchester, United Kingdom, 31 August–2 September 1988, pp. 189–192. The Plessey Company plc; available at <http://www.bmva.org/bmvc/1988/avc-88-023.pdf> (accessed August 2020).
20. Rosten E & Drummond T (2006) Machine learning for high-speed corner detection. In Proceedings of the European Conference on Computer Vision, Graz, Austria, 7–13 May 2006, pp. 430–443. Berlin: Springer; available at https://link.springer.com/chapter/10.1007/11744023_34 (accessed August 2020).
21. Bay H, Tuytelaars T & Gool LJV (2006) SURF: speeded up robust features. In Proceedings of the European Conference on Computer Vision, Graz, Austria, 7–13 May 2006, pp. 404–417. Berlin: Springer; available at https://link.springer.com/chapter/10.1007/11744023_32 (accessed August 2020).
22. Rahman SM (2009) *Food Properties Handbook*, 2nd ed. Boca Raton: CRC Press.